Experimental quantification of the impact of heterogeneous mix on thermonuclear burn

Brian Albright (balbright@lanl.gov)
Los Alamos National Laboratory

Thomas Murphy
Los Alamos National Laboratory https://orcid.org/0000-0002-6137-9873

M Douglas
Los Alamos National Laboratory

T Cardenas
Los Alamos National Laboratory

James Cooley
Los Alamos National Laboratory

Thomas Day
Los Alamos National Laboratory

Nicolas Denissen
Los Alamos National Laboratory

Carlos Stefano
Los Alamos National Laboratory https://orcid.org/0000-0001-6166-3519

Robert Gore
Los Alamos National Laboratory

M Gunderson
Los Alamos National Laboratory

Jeffrey Haack
Los Alamos National Laboratory

Brian Haines
Los Alamos National Laboratory https://orcid.org/0000-0002-3889-7074

Christopher Hamilton
Los Alamos National Laboratory https://orcid.org/0000-0002-1605-5992

Yongho Kim
Los Alamos National Laboratory

M Lee
Los Alamos National Laboratory

J Oertel
Los Alamos National Laboratory

R Olson

Los Alamos National Laboratory
R Randolph
Los Alamos National Laboratory
R Shah
University of Rochester
J Smidt
Los Alamos National Laboratory
Lin Yin
Los Alamos National Laboratory https://orcid.org/0000-0002-8978-5320

Article

Keywords: inertial confinement fusion (ICF), deuterium-tritium (DT), fuel

Posted Date: January 14th, 2021

DOI: https://doi.org/10.21203/rs.3.rs-135269/v1

Version of Record: A version of this preprint was published at Physics of Plasmas on February 1st, 2022.
See the published version at https://doi.org/10.1063/5.0082344.

Experimental quantification of the impact of heterogeneous mix on thermonuclear burn

Brian J. Albright[1], Thomas J. Murphy[1], Melissa R. Douglas[1], Tana Cardenas[1], James H. Cooley[1], Thomas H. Day[1], Nicholas A. Denissen[1], Carlos Di Stefano[1], Robert A. Gore[1], Mark A. Gunderson[1], Jeffrey R. Haack[1], Brian M. Haines[1], Christopher E. Hamilton[1], Yongho Kim[1], Matthew N. Lee[1], John A. Oertel[1], Richard E. Olson[1], Randall B. Randolph[1], Rahul C. Shah[2], Joseph M. Smidt[1] & Lin Yin[1]

[1]*Los Alamos National Laboratory, P.O. Box 1663, MS T087, Los Alamos, NM 87545, USA.*

[2]*Laboratory for Laser Energetics, University of Rochester, 250 E. River Rd., Rochester, NY 14623, USA.*

In inertial confinement fusion (ICF), deuterium-tritium (DT) fuel is brought to densities and temperatures where fusion ignition occurs. Mix of ablator material into the fuel may prevent ignition by diluting and cooling the fuel. MARBLE experiments at the National Ignition Facility (NIF) provide new insight into how mix affects thermonuclear burn. These experiments use laser-driven capsules containing deuterated plastic foam and tritium gas. Embedded within the foam are voids of known sizes and locations, which control the degree of heterogeneity of the fuel. Initially, the reactants are separated, with tritium concentrated in the voids and deuterium in the foam. During the implosion, mix occurs, leading to DT fusion reactions in the mixed region. Here we show that by measuring ratios of DT and deuterium-deuterium (DD) neutron yields for different macropore sizes and gas

compositions, effects of mix heterogeneity on thermonuclear burn may be quantified and understood for the first time.

ICF ignition involves compressing thermonuclear fuel to densities and temperatures where fusion heating exceeds losses from radiation, thermal conduction, and hydrodynamic work[1,2]. Achieving ignition has proven difficult, however, largely because of the presence of contaminant material in the fuel (mix). In ICF implosions, ablator material may mix into the fuel, diluting and cooling it, and reducing the rate of thermonuclear reactions[3-9]. This mix is not uniform and may be incomplete, as the time scale[10] for achieving a mixing transition[11], where flow drives the rapid development of atomic mixing, is comparable to the implosion time scales[12]. At present, the ability to predict how much mix occurs in ICF experiments, how this mix is distributed, and what the effects are on yield is limited. The MARBLE campaign addresses this by providing quantitative data for validating models and improving our understanding of the physics of mix and burn.

The degree to which mix affects yield depends on morphology, i.e., how heterogeneous the medium is at "bang time," the time of maximal yield production. Morphology is very difficult to diagnose directly in ICF settings, however. MARBLE was designed to study mix morphology and its effects on thermonuclear burn in ICF in a controlled way. In MARBLE, morphology is controlled through the use of capsules containing deuterated divinylbenzene (DVB) foam fabricated with "macropores," voids of known sizes and locations (see Figure 1), in which tritium gas resides. As the implosion progresses, a hierarchy of scales develops in the medium. At the finest scales, atomistic mix at the interfaces between tritium gas in the pores and deuterium in the foam

leads to DT reactions in the mixed regions. The smaller the macropore diameter, the more rapid and complete the mix at bang time and the higher the DT yield relative to the DD yield. (DD reactions in the interstitial foam plasma proceed in the absence of atomistic mix.)

In a volume V of homogeneously mixed fuel, the thermonuclear reaction rate is $\dot{R}_{\alpha\beta}^{hom} = \langle\sigma v\rangle_{\alpha\beta} N_\alpha N_\beta V^{-1}$, where for reactant species α and β, N_α and N_β are the respective numbers of particles in the burn volume V and $\langle\sigma v\rangle_{\alpha\beta}$ is the product of the fusion cross section σ and the relative velocity v averaged over the distribution functions of ion velocities of species α and β. In a separated reactants experiment such as MARBLE, the deuterium and tritium reactants are spatially separated initially. Heterogeneity leads to partial mixing of the deuterium and tritium, reducing the DT reaction rate relative to $\dot{R}_{DT}^{hom}$ while reducing somewhat the volume occupied by the deuterium and thus increasing the DD reaction rate relative to $\dot{R}_{DD}^{hom}$. The ratio of DT to DD yield would therefore be expected to be decrease with hetereogeneity.

Prior separated reactants experiments[13,14] studied mix in layered capsules containing deuterium with a tritium gas fill. These experiments suffer from ambiguity, however, as the mixing occurs far from the hot spot and uncontrolled, often poorly diagnosed hydrodynamic features complicate interpretations of the mixing dynamics. By the use of well characterized, macroporous foam throughout the burn volume, MARBLE avoids these issues.

Experimental Design

Our MARBLE experiments employ a two-shock implosion [15] on the National Ignition Facility (NIF) in a gas-filled hohlraum, a design shown to exhibit superior reproducibility[16]. In these experiments, a 1.2 MJ, 400 TW, 8 ns, two-shock laser pulse (Figure 2) was directed into a gold hohlraum to produce x-rays that were absorbed by the capsule ablator, leading to implosion of the capsule. The design desiderata include: 1) high x-ray conversion efficiency (85-90% of incident laser energy converted to x-rays); 2) low laser backscatter (<2%); 3) minimal hot electron production, which causes undesirable heating of the fuel (preheat) early in the implosion; and 4) implosion symmetry tuned through choice of laser cone fraction (i.e., without relying on cross-beam energy transfer, a nonlinear laser-plasma interaction process that is imperfectly understood[17,18]). This design led to hohlraum drive conditions that could be reliably calculated using integrated 2D rad-hydro simulations (laser + hohlraum + capsule) with the HYDRA radiation hydrodynamics code[19], as evidenced by our ability to predict simultaneously the time-resolved hohlraum x-ray drive, the capsule bang time, and the time-resolved capsule implosion symmetry. Further confidence in the design resulted from a series of shock-tube experiments on the Omega laser facility at the Laboratory for Laser Energetics that validated our understanding of shock propagation through fine-pore and engineered foams[20] as well as directly driven MARBLE capsule implosions on the Omega laser that were described well by simulations[12].

In our experiments, the target capsules consisted of 40 mg/cm^3 (the density volume-averaged over the macropores and interstitial foam matrix), engineered-pore-size, deuterated plastic foam inside machined silicone-doped plastic hemispheres that served as the ablator. The capsules were inserted into a 5.75 mm diameter, 9.44 mm long gold

hohlraum with a 0.3 mg/cm^3 helium fill gas and were filled by a fill tube with hydrogen-tritium (1.8 $\pm$ 1 mg/cm^3 HT, 5% T by atom) or argon-tritium (34 $\pm$ 1 mg/cm^3 ArT, 9% T by atom) gas mixtures at 7600 torr. The capsules were fielded at a temperature of 150 K to allow higher gas density at the set pressure. (Lower temperatures were not used in order to limit adsorption of hydrogenic species in the foam[21].)

The MARBLE experiments required synthesis of engineered, fully deuterated DVB foams with a tunable pore diameter from 10-90 microns. The engineered foams were made by dispersing hollow SiO_2 beads into an aerogel precursor, creaming the SiO_2 under gravity, polymerizing the dilute gel network in the interstitial regions, and etching the SiO_2 beads using hydrofluoric acid[22]. The process for synthesizing the foam is described in the Methods, along with a discussion of foam machining, fabrication of the capsules, and characterization of the targets, all of which proved critical for the reproducibility and analysis of our experiments.

Experimental Results

DD and DT neutron yields and inferred ion temperatures were measured for both the HT and ArT gas filled implosions. As shown in Figure 3, when a HT fill was used, ion temperatures for the DT and DD neutrons, obtained from the widths of the neutron time-of-flight (nToF) detector signals, were found to be quite different, with inferred ion temperatures from DT neutrons of around 3 keV, roughly twice the temperature of the inferred DD neutrons. In contrast, when ArT gas was used, the inferred DT ion temperatures dropped to around 1.6 keV and were in much better agreement with the DD ion temperatures (around 1.4 keV). Simulations indicate that this discrepancy is likely a

result of contributions of the initial shock yield, which occurs at higher temperature than the subsequent compression yield. The DT reactivity increases with temperature more quickly than does the DD reactivity, with the result that the burn-averaged ion temperature is weighted by shock yield more for the DT neutrons than for the DD neutrons, leading to a large observed temperature discrepancy. In contrast, for ArT implosions, radiative cooling of the shock flash nearly eliminates the shock yield, so both DD and DT inferred ion temperatures are representative of the ion temperature during the compression yield. This behavior is observed both in simulations and in time-resolved x-ray emission data from the Streaked Polar Instrumentation for Diagnosing Energetic Radiation (SPIDER) diagnostic[23] on the NIF shown in Figure 3. Data are shown for NIF shots N198729-001 and N181028-002, which are representative of the observed behavior of HT and ArT gas fills, respectively. X-ray emission from the capsule with an HT gas fill shows two peaks, associated with shock flash and compression, whereas emission from the capsule with an ArT fill has negligible shock flash and only a compression yield peak.

To analyze the effects of mix morphology for different macropore sizes and gas fills, we compared the ratio of DT to DD neutron yield normalized by twice the tritium density divided by the deuterium density, a quantity we refer to as *normalized yield ratio* (NYR). Use of NYR allowed us to control for variations in foam density and gas composition and density and to decrease systematic variability from shot-to-shot variation. For uniform atomic mix at a single ion temperature, NYR should be equal to the ratio of DT to DD reaction rates at the hot spot temperature at bang time.

Heterogeneity (partial mixing) would be expected to produce a lower NYR in the absence of species separation.

In experiments with the ArT gas fill, the NYR decreased from the atomically mixed value for fine pore foam to a lower value, consistent with our expectations for heterogeneous mix (Figure 4). For capsules with an HT gas fill, however, the expected decrease in NYR with increasing macropore diameter was not observed. Instead, the data may show a slight *increase* in NYR. This behavior may be a result of thermal fluctuations brought on by complicated material distributions with unequilibrated contaminants in the pore plasma, a feature observed in high-resolution calculations of similar experiments fielded on the Omega laser system at the Laboratory for Laser Energetics[12]. (In contrast, for ArT fills, the presence of argon enhances thermal conductivity and reduces the time scale for thermal equilibration, preventing significant temperature nonequilibration.) The HT fill experiments were also much more susceptible to preheat from non-thermal M-band radiation from the hohlraum walls and radiation from the shocks in the foam, leading to violent expansion of the foam material, compression of the macropores prior to compression burn, and the possibility of substantial hydrodynamic stirring prior to bang time, all of which would increase the NYR. A comparison of high-resolution three-dimensional radiation hydrodynamics simulations (described in the next section) confirm these differences for ArT and HT fills, the former showing, e.g., 82% less pore compression from M-band preheat. Moreover, in the HT fill experiments, lower mean ion charge states and smaller collapsed macropore diameters lead to mean-free-paths of the reactant ions being comparable to the diameters of the pores after preheat, introducing the

possibility of Knudsen-layer[24-26] and other plasma kinetic effects[27,28] on thermonuclear burn rates.

Numerical Modeling

Numerical simulations have proven invaluable in interpreting our experiments. We obtained from integrated two-dimensional HYDRA simulations a time- and symmetry-resolved frequency dependent radiation source (FDS source) that was used as a drive input for capsule implosion simulations using the LANL xRAGE code[9,29]. This enabled comparison with both high-resolution calculations of the implosion, which resolve the as-shot geometry of the macropores and other features of the assembly, as well as calculations at lower resolutions and dimensions that employ statistical treatments of the mix and its effects on thermonuclear burn.

Two high-resolution, three-dimensional, xRAGE simulations, one with an HT fill and another, ArT fill, were performed of MARBLE implosion N180729, which had 90-micron pores and an HT gas fill. The simulations employed full physics with initial conditions that included accurate representations of the fill tube geometry as well as the glue-filled gap between the CH hemispheres used to surround the foam. Additionally, the initial conditions included an accurate representation of the engineered foam: the location, geometry, and size of every macropore as well as residual pieces of glass in the as-shot capsule were characterized by x-ray tomography and faithfully reproduced in the initial conditions. The distributions of materials in the HT capsule implosion are shown in Figure 5 at t=0, 7.9 ns, 8.1 ns (shock flash), and 8.35 ns (compression burn). The shell (shown in the left panel) is red, the HT-filled pores are green, the glue is yellow, the glass

(from both the fill tube and residual material from foam fabrication) is blue, the position of the shock front is magenta, and the burn region with ion temperature $T_i > 1$ keV is cyan. The shock front and burn region have a P4 asymmetry resulting from the glue joint between the hemispheres (the glue has higher density than the ablator and slows the shock somewhat near the equator). The inner shell radius is 705 microns at t=0 and 270 microns at t=7.9 ns. The burn volume has radius 80 microns. By 7.9 ns, the pores have collapsed from heating of the foam, caused primarily by radiative emission from the shock front, and the right panel shows the effect of the shock interaction with the pores behind the shock front. In contrast, high-resolution simulations of the same capsule with an ArT gas fill instead of HT show that the presence of Ar increases substantially the electron pressure and prevents pore collapse. In both, the thick shell and high-density capsule fill prevent detrimental effects from the fill tube and the capsule seam, though some mild jetting of glass material from the fill tube is evident at 7.9 ns. As shown in Figures 3 and 4, the simulated burn-weighted ion temperatures (BWTI) and NYR were in good agreement with the data. The difference in BWTI is dominated by the different temperatures from shock and compression yields. The DT and DD BWTI remain the same during shock flash and though temperature separation as in Refs.[12,30] is observed during compression burn (757 eV in the gas and 735 eV in the foam matrix), the effect of this separation is minor compared with temporal variations in BWTI.

High resolution, three-dimensional simulations are impractical for ICF design, which requires rapid turn-around. One must instead rely on models that treat the mix statistically. In the xRAGE code, this is done by employing the Besnard-Harlow-Rauenzahn (BHR) 3.1 Reynolds-Averaged Navier Stokes (RANS) model for turbulent

mixing[31,32] with a probability distribution function (PDF) burn model that accounts for the effects of heterogeneous mix using moments of the probability distribution functions of the concentrations of reacting species[33]. (The mix model was not used in the high-resolution simulations.) In xRAGE, the thermonuclear reaction rate[34,35] is modified according to

$$\dot{R}_{\alpha\beta} = \dot{R}_{\alpha\beta}^{hom}\left[1 - \frac{\overline{\rho'^2}}{\bar{\rho}^2}\left(\frac{1+r}{r\tilde{c}_1\tilde{c}_2}\right)\right], \qquad (1)$$

where $\tilde{c}_1$ and $\tilde{c}_2$ are mass-weighted Favre average concentrations of the mixing materials, $\bar{\rho}$ is the Reynolds-average density of the mixed fluid, $\overline{\rho'^2}$ is the variance of this density, $r = \rho_2/\rho_1 - 1$, and α and β indicate the reacting species (deuterium and tritium) which are components of the mixing fluids. To account for changes in mix morphology, the BHR 3.1 mix model evolves the density-specific volume covariance $b = -\langle(\rho - \bar{\rho})(\rho^{-1} - \bar{\rho}^{-1})\rangle$, where brackets denote an ensemble average. This quantity encodes the heterogeneity of the medium, making it possible to compute $\overline{\rho'^2}/\bar{\rho}^2$ in Equation (1)[32] and modify the thermonuclear reaction rates accordingly.

In a hydrodynamic description of the plasma, assuming the reactants are in thermal equilibrium, dividing the NYR by the expected NYR for homogeneous mix gives a quantity from 0 to 1 known as the *mixedness* of the medium over the burn interval. The mixedness for the ArT and HT experiments is shown in Figure 6 as a function of macropore diameter. The data are compared with the mixedness obtained from numerical simulations using the BHR model for turbulent mixing with a PDF burn fusion reactivity. The BHR model was initialized with a turbulent scale length S_0, a model parameter that we set equal to the macropore diameter d_{pore} times a scaling factor. As shown in Figure 6, the MARBLE ArT results are in good quantitative agreement with the use of a scaling

factor of 0.07, corresponding to an S_0 of size roughly that of the radial size of the macropores after compression by the main shock as it passes through the foam. In contrast, the sub-grid mix model fails to explain the HT inferred mixedness data, even qualitatively, evidencing no reduction of mixedness with pore size. (If anything, the data show a slight increase.) This is an indication of missing physics from the modeling or invalid assumptions in computing the mixedness. In this case, preheat in the HT experiments from non-thermal M-band radiation from the hohlraum and radiation emanating from the shock may have caused vigorous mixing prior to bang time, obviating the dependence of yield on initial inhomogeneity. (By virtue of their higher opacity and higher electron pressure in the macropores, capsules with ArT fills would be much less susceptible to preheat-induced mixing.)

Discussion

MARBLE experiments allow for the first time a detailed study of the effects of mix morphology on thermonuclear burn, a problem crucial to the success of ICF ignition. By varying macropore size (the degree of initial heterogeneity) and gas fill (the ion mean free paths), MARBLE experiments enable experimental control of the degree of mix morphology as well as of the introduction of effects such as ion temperature non-equilibration and plasma kinetic behavior.

This platform enables a rigorous test of computational models of mix and burn. Comparisons with mix and burn models in the LANL xRAGE code show quantitative agreement with the ensemble of ArT fill data for a common, fixed ratio of turbulent scale length to macropore diameter. However, the inability of this model to match the HT fill

data raises questions about how well we understand how hydrogenic plasmas mix with carbon (e.g., ablator mix into DT ice in ICF settings). Such mix affects compressibility and fuel ρR, both long-standing issues in ICF, and an improved understanding of the interplay of mix and burn will therefore have important implications for predicting ICF fusion experiments on the NIF.

Methods

Synthesis of Fully Deuterated Foam

Deuterium labeled styrene was copolymerized with fully deuterated 1,4-divinylbenzene, synthesized by the following method: First, 1,4-dibromobenzene D4 (deuterated para-dibromobenzene) was subjected to Sonogashira coupling with 2 equivalents of trimethylsilyl acetylene. The trimethylsilyl groups were then removed with potassium fluoride in D labeled methanol. Finally, a Lindlar type catalyst (Pd nanoparticles on carbon) with bubbled deuterium gas was used to reduce the acetylene groups to vinyl groups. The final product, 1,4 divinylbenzene D10 was obtained in about 70% yield. The level of deuteration was measured using Nuclear Magnetic Resonance (NMR).

Target Machining

For experiments at Omega and the NIF, 20- and 120-micron-thickness capsules were machined and the engineered joint was sealed with Epon 815C adhesive, chosen for its high adhesive strength. After the sleeves and mandrels were glued together, the assembly was cured for several days at room temperature to prevent adhesive

shrinkage[36]. Machining the foam sphere required a new dry machining method developed using turn milling[37] to avoid difficulties with wax fill (e.g., non-uniform shrinkage and incomplete removal of the wax[38]).

Foam Characterization

Control of systematic errors in the MARBLE experiments required accurate foam characterization[39], including precise measurements of the tritium and deuterium content. The former was obtained from measuring capsule pressure and temperature just before shot time. The latter required pre-shot characterization of the foam density, measured gravimetrically and with x-ray adsorption, and the deuterium fraction, measured by nuclear magnetic resonance. The heterogeneity arises from the macropore structure, so the size distribution and volume fraction of the macropores must be known precisely. This information was obtained using Scanning Electron Microscopy and computed tomography. Impurities, such as silicon left in the foam as a result of incomplete etching of the glass microballoons used to form the macropores, was characterized using confocal x-ray fluorescence. Finally, pressure and temperature ranges for fielding experiments are affected by the foam's ability to hold excess amounts of hydrogenic species through surface adsorption. Therefore, the specific surface area of the foam must be measured and its ability to hold hydrogen, characterized through nitrogen gas sorption porosimetry measurements. Previous experiments utilizing a single-shock pulse with fine-pore foam at different temperatures and pressures support the calculations that indicate that the effect of surface adsorption was minimal at the conditions used in the experiments reported here. In these experiments, an initial implosion (N170625-002) was fielded at

room temperature, followed by an implosion (N170713-004) with the same fill gas density, and then (N180313-001) with twice the fill gas density. The normalized yield ratios for the three were all within 11% of the average, and the room temperature implosion and high gas density shots had normalized yield ratios with 3% of each other.

xRAGE simulations

The large-scale xRAGE simulations were run with a maximum resolution of 0.25 microns using initial conditions obtained from x-ray tomography of the "as built" capsules, accounting for macropore locations and orientations, inclusions of incompletely etched SiO_2, and the joint feature from assembly. This level of fidelity is enabled by xRAGE's adaptive mesh refinement (AMR). The resulting simulations used between 5.6 and 11.4 billion cells and more than 400 million CPU hours on Lawrence Livermore National Laboratory's Sequoia and Sierra supercomputers.

Measures of mix

Assuming a mixture of D and T, the neutron yield is dependent on the average of the products of the densities of D and T $Y_{DT} = \langle n_D n_T \rangle \langle \sigma v \rangle_{DT} V\tau$. In general, $\langle n_D n_T \rangle \leq \langle n_D \rangle \langle n_T \rangle$. and we can define the mixedness $\theta \in [0,1]$ such that $\langle n_D n_T \rangle = \langle n_D \rangle \langle n_T \rangle \theta$. We can measure both the DT and DD neutron yields, given by:

$$Y_{DT} = \langle n_D n_T \rangle \langle \sigma v \rangle_{DT} V_{DT} \tau_{DT}$$

$$Y_{DD} = \frac{1}{2} \langle n_D^2 \rangle \langle \sigma v \rangle_{DT} V_{DD} \tau_{DD}$$

If we assume that the burn volume and burn time for the two reactions are approximately equal, the ratio of yields is given by

$$\frac{Y_{DT}}{Y_{DD}} = 2\theta \frac{\langle n_D \rangle \langle n_T \rangle}{\langle n_D^2 \rangle} \frac{\langle \sigma v \rangle_{DT}}{\langle \sigma v \rangle_{DT}}$$

It can be shown that for the target parameters used in these experiments, $\langle n_D^2 \rangle \approx \langle n_D \rangle^2$, which allows us to write

$$\frac{1}{2} \frac{\langle n_D \rangle}{\langle n_T \rangle} \frac{Y_{DT}}{Y_{DD}} = \theta \frac{\langle \sigma v \rangle_{DT}}{\langle \sigma v \rangle_{DT}}$$

We refer to the term on the left as the normalized yield ratio (NYR). For uniformly atomic mix, NYR is equal to the reaction rate ratio at a given temperature, and is less by a factor of θ for heterogeneous mix. Dividing the NYR by the reaction rate ratio then provides a measure of the mixedness. The uncertainty in the mixedness is dependent on uncertainties in measurement of the ion temperature (from neutron time-of-flight), the yield for each reaction, the deuterium and tritium densities, and the degree to which the burn volumes and burn times for the two reactions are indeed equal.

Acknowledgements

The authors thank J. Cobble and J. Fincke for contributions to the development of the MARBLE platform, P. Donovan, L. Goodwin, L. Kuettner, T. Quintana, D. Schmidt, A. Strickland, C. Wilson, B. Patterson, and J. Cowen for contributions to target fabrication and characterization, General Atomics for performing GDP coating and characterization of final targets, LLNL's NIF laser facility operations for laser operation and technical support, LLNL's computing support for supercomputer operations and support, and LANL's Eulerian Applications Project (in particular, M. Daniels, M. McKay, and A. Nelson) for xRAGE support. This work was performed under the auspices of the US

DOE by LANL under contract numbers DE-AC52-06NA25396 and 89233218NCA000001.

Author contributions

T.J.M. conceived the idea for these experiments. B.J.A. and M.R.D. led the campaign. R.E.O. designed the experiments. T.J.M, Y.K., R.C.S. executed the experiments. B.M.H., M.A.G., J.M.S., R.E.O., C.D.S. performed and analyzed rad-hydro calculations to interpret the experiments. Y.K., T.J.M., and R.S. executed supporting Omega experiments. N.A.D., R.A.G., and B.M.H. provided expertise on mix modeling. T.C., T.H.D., C.E.H., M.N.L., J.A.O., and R.B.R. developed the targets. B.J.A., J.H.C., J.R.H., and L.Y. assessed kinetic effects. B.J.A., B.M.H., R.C.S., M.R.D., M.A.G., Y.K., T.J.M., R.E.O., and R.A.G. analyzed and interpreted the experimental and simulation results. All of the authors contributed to the writing of the manuscript.

Competing Interests

The authors declare that they have no competing financial interests.

Correspondence

Correspondence and requests for materials should be addressed to B.J.A. (email: balbright@lanl.gov).

References

1. Nuckolls, J., Wood, L., Thiessen, A. & Zimmerman, G. Laser compression of matter to super-high densities: CTR applications. *Nature* **2** , 139–142 (1972).

2. Edwards, M. J. et al. Progress towards ignition on the National Ignition Facility. *Phys. Plasmas* **20**, 070501 (2013)

3 Regan, S. P. et al. Hot-spot mix in ignition-scale implosions on the NIF. *Phys. Plasmas* **19**, 056307 (2012).

4 Ma, T. et al. Onset of hydrodynamic mix in high-velocity, highly compressed inertial confinement fusion implosions. *Phys. Rev. Lett.* **111**, 085004 (2013).

5 Regan, S. P. et al. Hot-spot mix in ignition-scale inertial confinement fusion targets. *Phys. Rev. Lett.* **111**, 045001 (2013).

6 Ma, T. et al. The role of hot spot mix in the low-foot and high-foot implosions on the NIF. *Phys. Plasmas* **24**, 056311 (2017).

7 Clark, D. S. et al. Short-wavelength and three-dimensional instability evolution in National Ignition Facility ignition capsule designs. *Phys. Plasmas* **18**, 082701 (2011).

8 Clark, D. S. et al. Three-dimensional simulations of low foot and high foot implosion experiments on the National Ignition Facility. *Phys. Plasmas* **23**, 056302 (2016).

9 Haines, B. M., Aldrich, C. H., Campbell, J. M., Rauenzahn, R. M. & Wingate, C. A. High-resolution modeling of indirectly driven high-convergence layered inertial confinement fusion capsule implosions. *Phys. Plasmas* **24**, 052701 (2017).

10 Zhou, Y. Unification and extension of the similarity scaling criteria and mixing transition for studying astrophysics using high energy density laboratory experiments or numerical simulations. *Phys. Plasmas* **14**, 082701 (2007).

11 Dimotakis, P. E. The mixing transition in turbulent flows. *J. Fluid Mech.* **409**, 69–98 (2000).

12 Haines, B. M. et al., Observation of persistent species temperature separation in inertial confinement fusion mixtures. *Nature Communications* **11**, 544 (2020).

13 Wilson, D. C. et al. Atomic mix in directly driven inertial confinement implosions. *Phys. Plasmas* **18**, 112707 (2011).

14 Smalyuk, V. A. et al. Measurements of an Ablator-Gas Atomic Mix in Indirectly Driven Implosions at the National Ignition Facility. *Phys. Rev. Lett.* **112**, 025002 (2014).

15 Olson, R. E et al., Development of the Marble Experimental Platform at the National Ignition Facility. *Phys. Plasmas* **27**, 102703 (2020).

16 Khan, S. F. et al. Symmetry tuning of a near one-dimensional 2-shock platform for code validation at the National Ignition Facility. *Phys. Plasmas* 23, 042708 (2016).

17 Town, R. J. P. et al. Analysis of the National Ignition Facility ignition hohlraum energetics experiments. *Phys. Plasmas* **18**, 056302 (2011).

18 Michel, P. et al. Stochastic ion heating from many overlapping laser beams in fusion plasmas. *Phys. Rev. Lett.* **109**, 195004 (2012).

19 Marinak, M. M et al., Three-dimensional HYDRA simulations of National Ignition Facility targets. *Phys. Plasmas* **8**, 2275 (2001).

20 Kim, Y. et al., Experimental validation of shock propagation through a foam with macro-pores. *Phys. Plasmas* (in press).

21 Germain J., Hradil, J., Fréchet, J. M. J., & Svec, F., High surface area nanoporous polymers for reversible hydrogen storage. *Chem. Mater*. **18**, 4430 (2006).

22 Hamilton, C.E., Lee, M. N., & Parra-Vasquez, N. G., Development of Heirarchical, Tunable Pore Size Polymer Foams for ICF Targets. *Fusion Science and Technology* **70**, 226-229 (2016).

23 Khan, S. F. et al., Measuring x-ray burn history with the Streaked Polar Instrumentation for Diagnosing Energetic Radiation (SPIDER) at the National Ignition Facility (NIF). *Proc. SPIE 8505, Target Diagnostics Physics and Engineering for Inertial Confinement Fusion,* 850505 (15 October 2012); https://doi.org/10.1117/12.930032

24 Molvig, K., Hoffman, N. M., Albright, B. J., Nelson, E. M. & Webster, R. B., Knudsen layer reduction of Fusion Reactivity. *Phys. Rev. Lett*. **109**, 095001 (2012).

25 Albright, B. J et al., Revised Knudsen layer reduction of Fusion Reactivity. *Phys. Plasmas* **20**, 122705 (2013).

26 Cohen, B. I., Dimits, A. M., Zimmerman, G. B. & Wilks, S. C., One-dimensional particle simulations of Knudsen-layer effects on D-T fusion. *Phys. Plasmas* **21**, 122701 (2014).

27 Rinderknecht, H. G., Amendt, P. A., Wilks, S. C. & Collins, G., Kinetic physics in ICF: present understanding and future directions. *Plasma Physics and Controlled Fusion* **60**, 064001 (2018).

28 Yin, L. et al., Plasma kinetic effects on interfacial mix and burn rates in multispatial dimensions. *Phys. Plasmas* **26**, 062302 (2019).

29 Gittings, M et al. The RAGE radiation-hydrodynamic code. *Comput. Sci. Discov*. **1**, 015005 (2008).

30 Haines, B. M. et al., The rate of development of atomic mixing and temperature equilibration in inertial confinement fusion implosions. *Phys. Plasmas* **27**, 102701 (2020).

31 Besnard, D., Harlow, F. H., Rauenzahn, R. M. & Zemach, C. Turbulence transport equations for variable-density turbulence and their relationship to two-field models, Tech. Rep. LA-12393- MS, Los Alamos National Laboratory, available from the U. S. Department of Energy, Office of Scientific and Technical Information, P.O. Box 62, Oak Ridge, TN 37831. (1992).

32 Banerjee, A., Gore, R. A. & Andrews, M. J., Development and validation of a turbulent-mix model for variable-density and compressible flows. *Phys. Rev. E* **82** 046309 (2010).

33 Ristorcelli, J. R., Exact statistical results for binary mixing and reaction in variable density turbulence, Phys. Fluids 29 (2017) 020705.

34 Denissen, N. A. & Ristorcelli, J. R., Modeling reaction rates in variable-density turbulent mixing, Tech. Rep. LA-UR-14-28935, Los Alamos National Laboratory (2014).

35 Murphy, T. J. et al. Results from single-shock Marble experiments studying thermonuclear burn in the presence of heterogeneous mix on the National Ignition Facility. *High Energy Density Physics* (submitted).

36 Randolph, R. B et al., Process Development and Micro-Machining of MARBLE Foam-Cored Rexolite Hemi-Shell Ablator Capsules. *Fusion Sci. and Technology*, **70**(2), 230-236 (2016).

37 Randolph, R. B. et al., Dry-Machining of Aerogel Foams, CH Foams, and Specially Engineered Foams Using Turn-Milling Techniques. *Fusion Sci. and Technol*. **73**(2), 230-236 (2017).

38 Cluff, K. J., Goodwin, L. A., Hamilton, C. E., Lee, M. N., & Oertel, J. A., Quantitative Determination of Wax Contamination in Polystyrene HIPE Foam Using Solid-State NMR. *Fusion Sci. and Technology* **73**(2), 183-186 (2017).

39 Cardenas, T et al., Material Characterization of Hierarchical Tunable Pore Size Polymer Foams used in the MARBLE mix morphology experiment. *Fusion Sci. and Technol*. **8**, 1-12 (2020) doi.org/10.1080/15361055.2020.1790713.

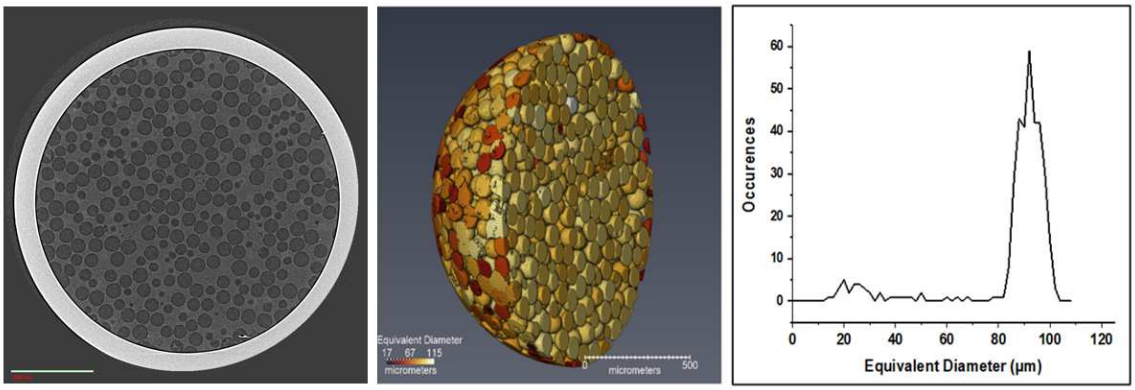

Figure 1 Tomographic analysis of a MARBLE capsule containing 90 micron macroporous foam.

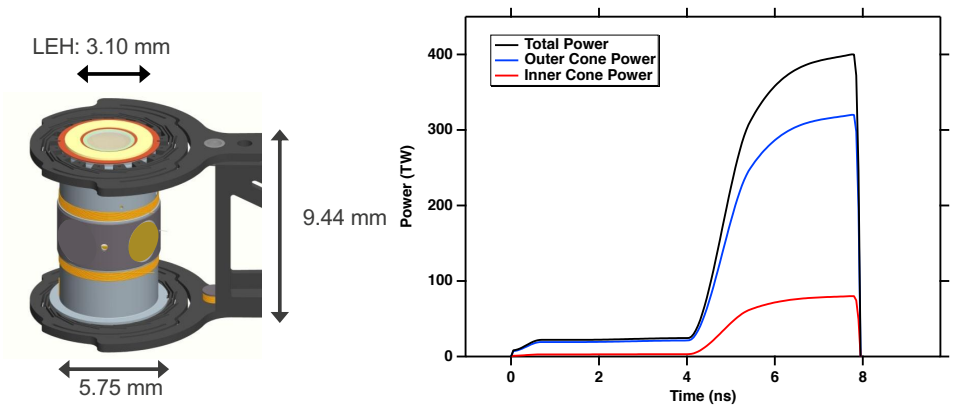

Figure 2 (Left) Hohlraum geometry for MARBLE experiments. (Right) Laser pulse shape used to drive the Marble two-shock targets.

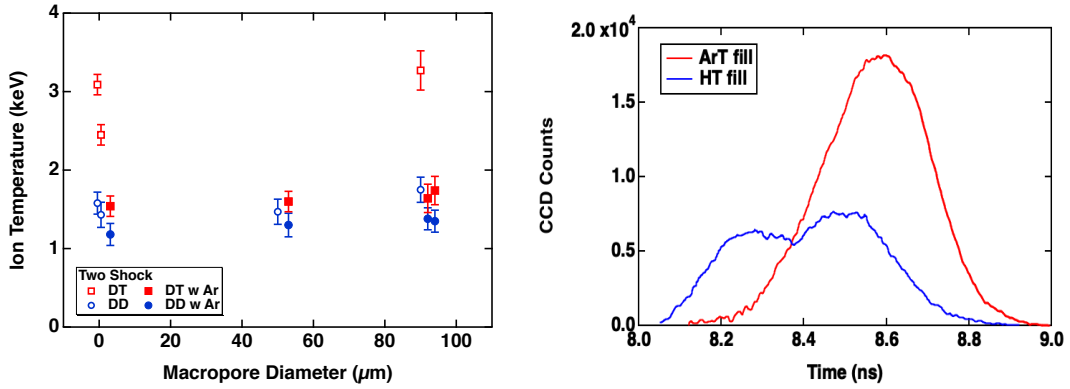

Figure 3 (Left) Burn-weighted ion temperatures from the DD (circle) and DT (square) nToF data for HT gas fill (open) and ArT gas fill (filled) implosions. With the HT fills, the DT and DD ion temperatures were very different. With the ArT fills, they are in agreement. (Right) X-ray emission from HT (blue) shows a two-humped emission, consistent with shock flash and compression yields. The ArT (red) shows only a single hump associated with compression yield.

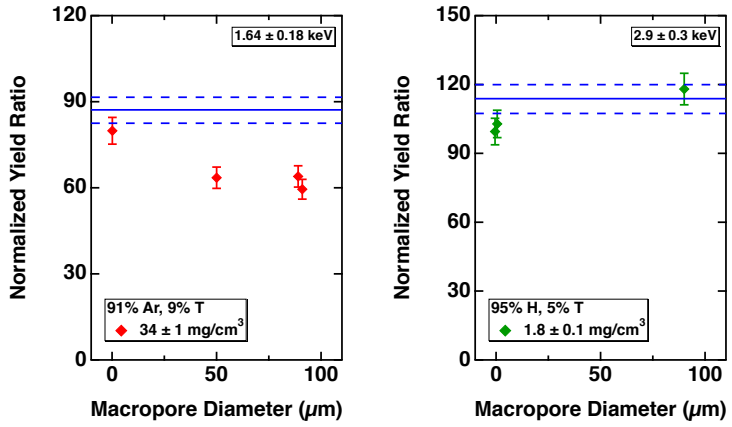

Figure 4 Normalized DT/DD yield ratio vs macropore diameter for (left) argon/tritium and (right) hydrogen/tritium gas fill. The blue lines show the expected ratio for uniform atomic mix for the range of ion temperatures inferred from DT nToF broadening.

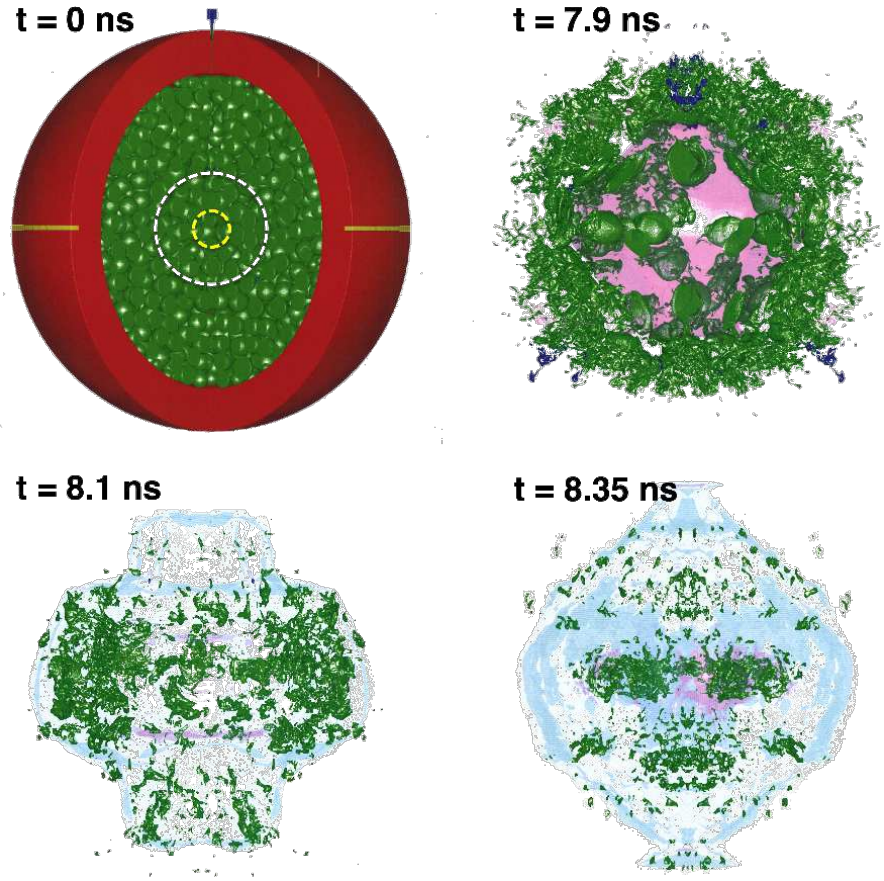

Figure 5 Distributions of materials from xRAGE simulations of MARBLE implosion N180729, which had 90 μm pores and an HT gas fill. The shell is red, the HT-filled pores are green, the glue is yellow, the glass is blue, the shock front (upper right panel) is magenta, and the burn volume (lower left, at shock flash time; lower right, at compression burn) is cyan. For scale, the upper right and lower images reside within the white and yellow dashed regions, respectively.

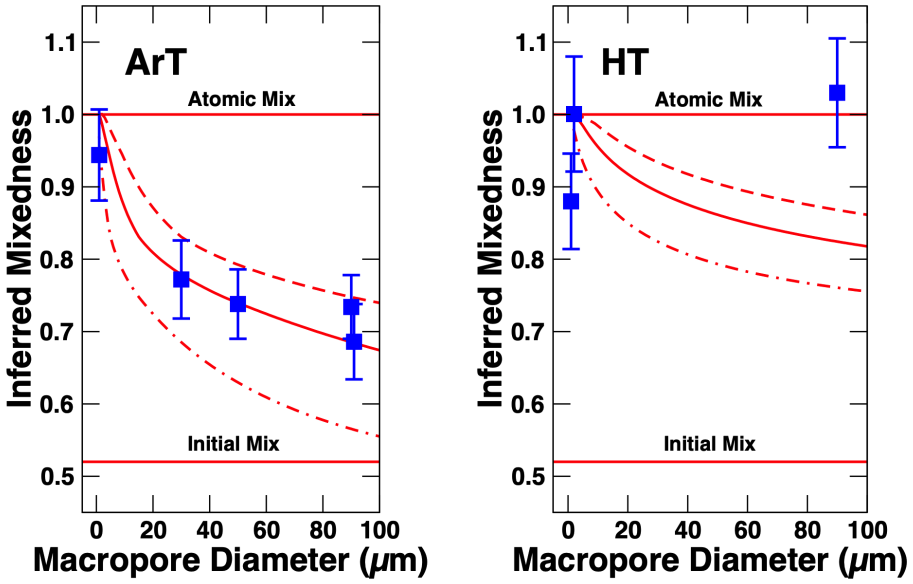

Figure 6 Inferred mixedness data (blue squares) for ArT and HT experiments as a function of macropore diameter d_{pore}. Also shown are simulated results with three relations of the turbulent scale length S_0 in the BHR mix model to d_{pore}: $S_0 = 0.07d_{pore}$ (solid curve), $S_0 = 0.03d_{pore}$ (dashed), and $S_0 = 0.2d_{pore}$ (dot-dashed). For uniform atomic mix, the mixedness is unity. Initial mix assumes that the gas within the foam mixes with the foam, but that the gas in the macropores remains separated.

Figures

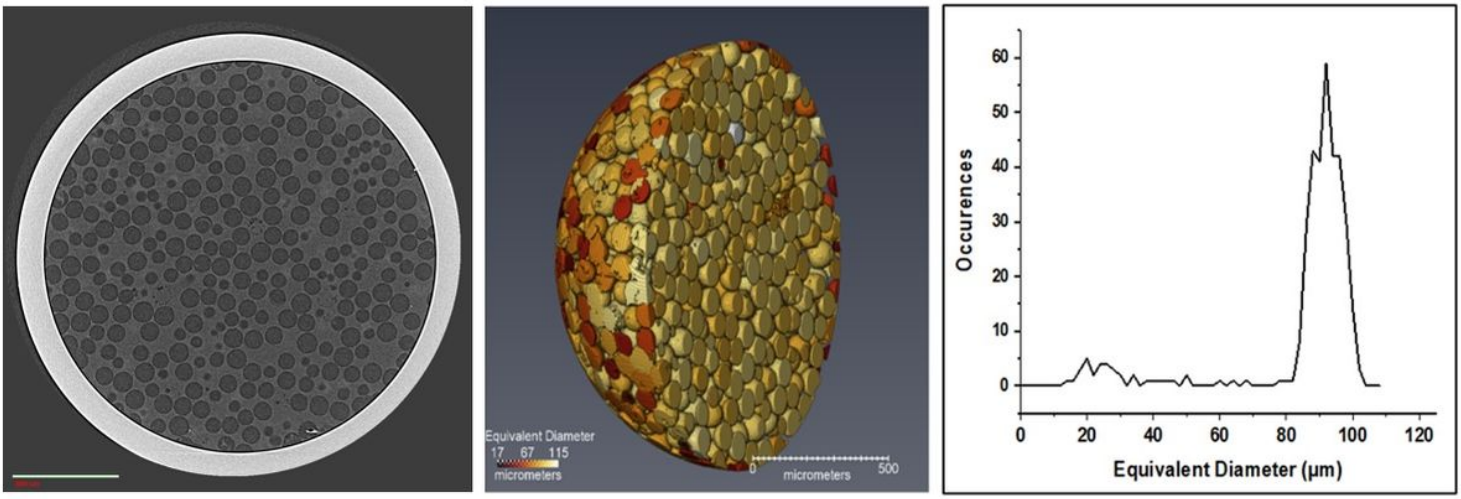

Figure 1

Tomographic analysis of a MARBLE capsule containing 90 micron macroporous foam.

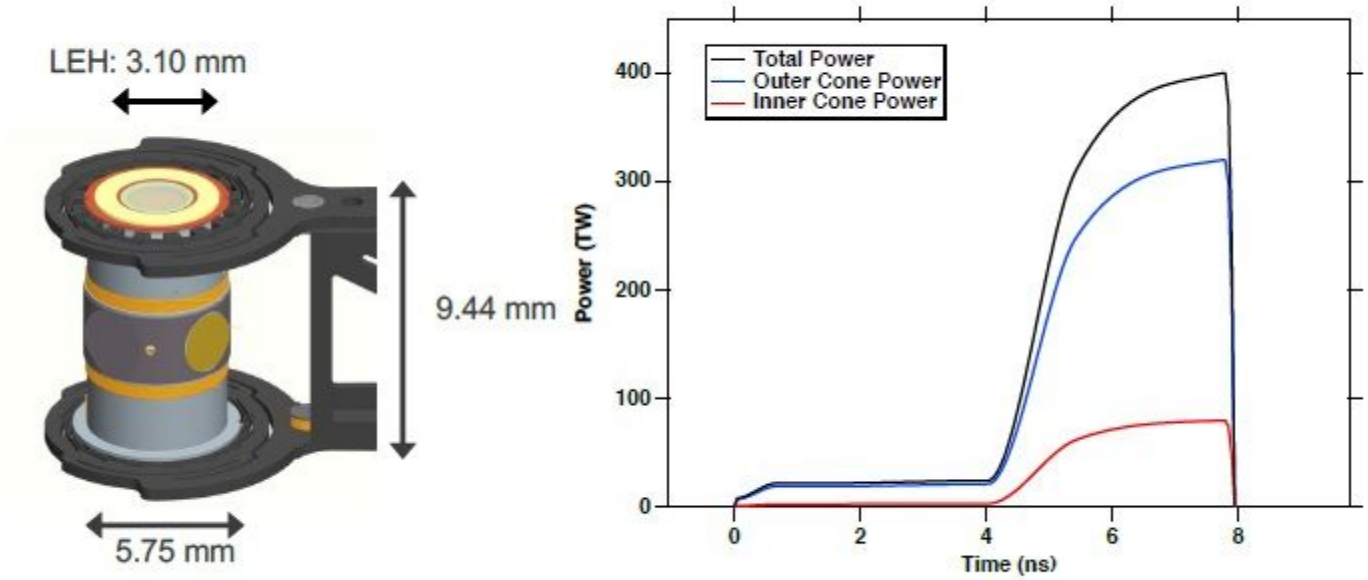

Figure 2

(Left) Hohlraum geometry for MARBLE experiments. (Right) Laser pulse shape used to drive the Marble two-shock targets.

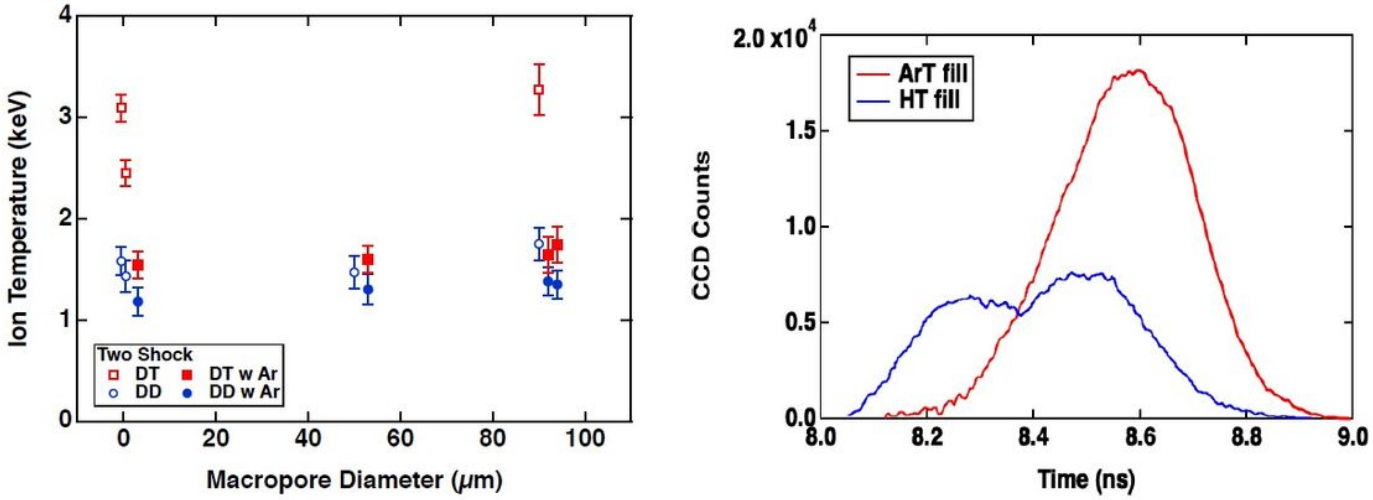

Figure 3

(Left) Burn-weighted ion temperatures from the DD (circle) and DT (square) nToF data for HT gas fill (open) and ArT gas fill (filled) implosions. With the HT fills, the DT and DD ion temperatures were very different. With the ArT fills, they are in agreement. (Right) X-ray emission from HT (blue) shows a two humped emission, consistent with shock flash and compression yields. The ArT (red) shows only a single hump associated with compression yield.

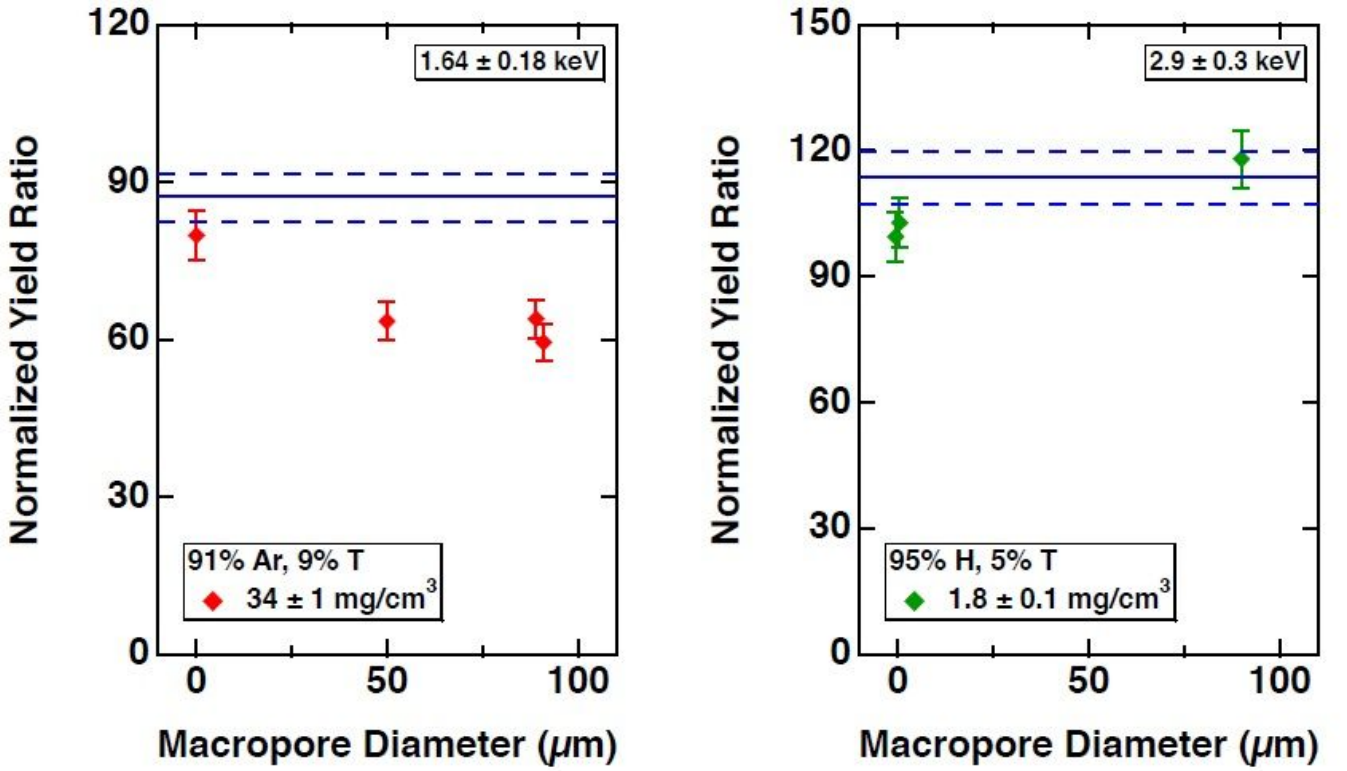

Figure 4

Normalized DT/DD yield ratio vs macropore diameter for (left) argon/tritium and (right) hydrogen/tritium gas fill. The blue lines show the expected ratio for uniform atomic mix for the range of ion temperatures inferred from DT nToF broadening.

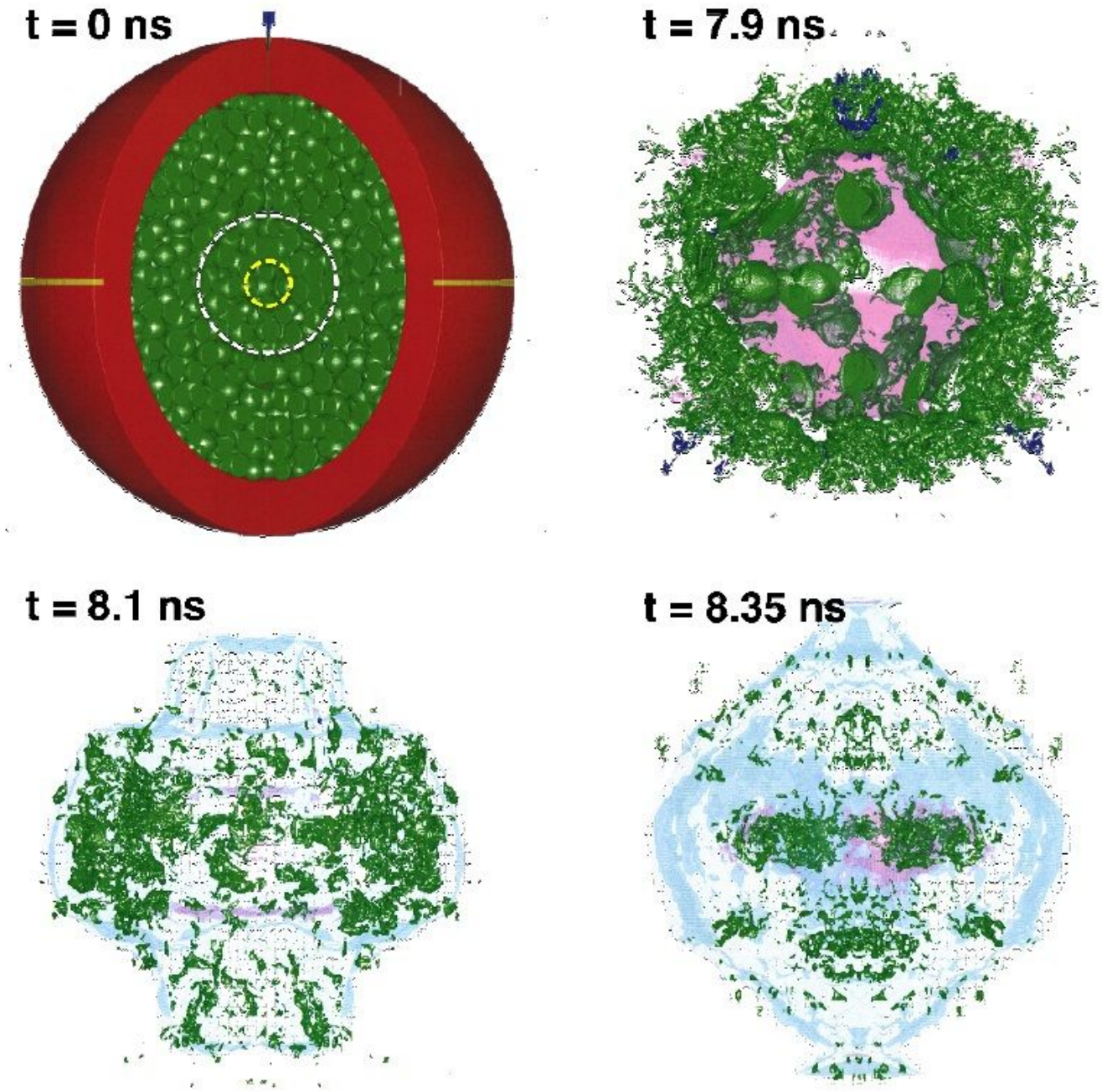

Figure 5

Distributions of materials from xRAGE simulations of MARBLE implosion N180729, which had 90 μm pores and an HT gas fill. The shell is red, the HT-filled pores are green, the glue is yellow, the glass is blue, the shock front (upper right panel) is magenta, and the burn volume (lower left, at shock flash time; lower right, at compression burn) is cyan. For scale, the upper right and lower images reside within the white and yellow dashed regions, respectively.

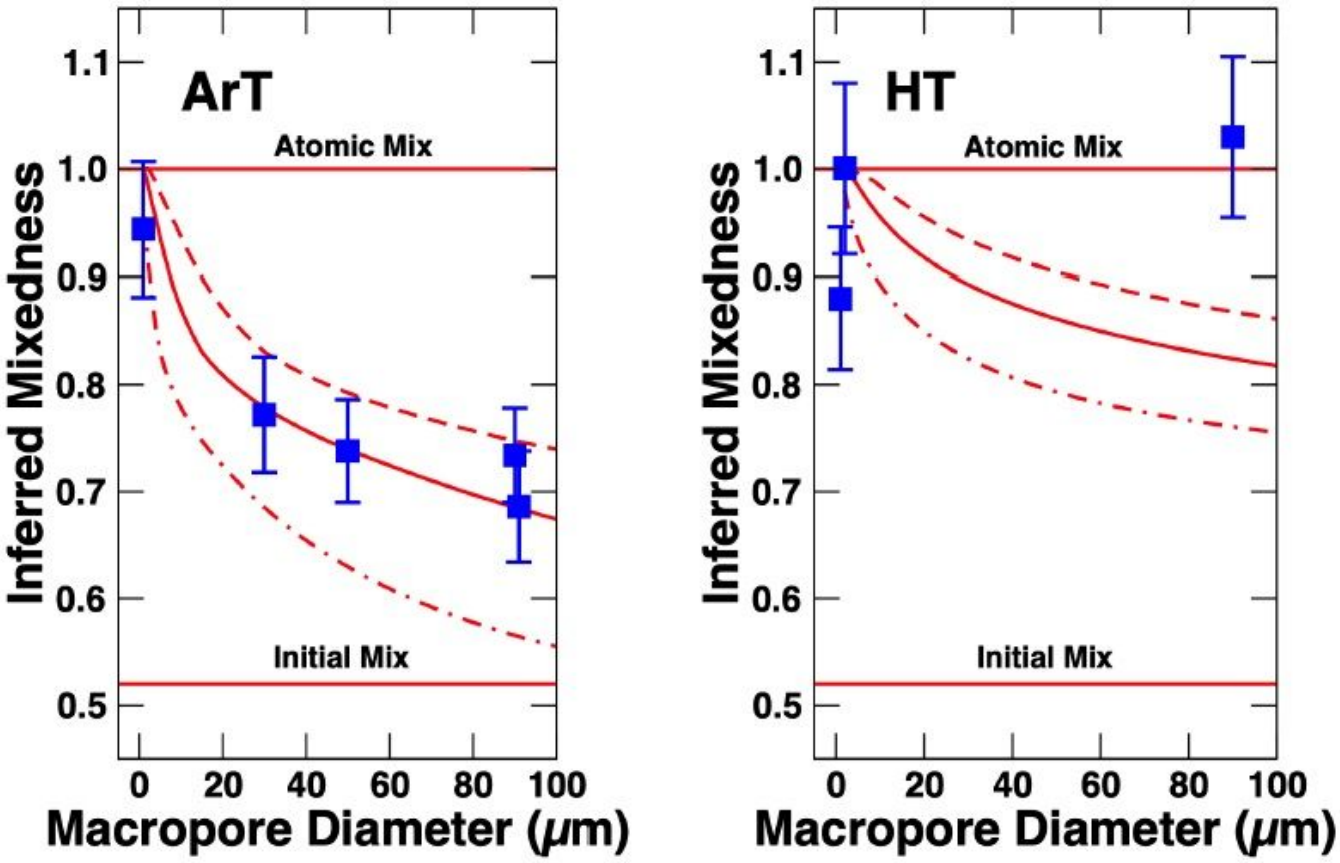

Figure 6

Inferred mixedness data (blue squares) for ArT and HT experiments as a function of macropore diameter dpore. Also shown are simulated results with three relations of the turbulent scale length S0 in the BHR mix model to dpore: S0 = 0.07dpore (solid curve), S0 = 0.03dpore (dashed), and S0 = 0.2dpore (dot-dashed). For uniform atomic mix, the mixedness is unity. Initial mix assumes that the gas within the foam mixes with the foam, but that the gas in the macropores remains separated.